ARTICLE IN PRESS

Available online at www.sciencedirect.com

SCIENCE DIRECT®

Journal of Non-Crystalline Solids xxx (2003) xxx–xxx

JOURNAL OF NON-CRYSTALLINE SOLIDS

www.elsevier.com/locate/jnoncrysol

Surface chemistry and trimethylsilyl functionalization of Stöber silica sols

T.I. Suratwala *, M.L. Hanna, E.L. Miller, P.K. Whitman, I.M. Thomas, P.R. Ehrmann, R.S. Maxwell, A.K. Burnham

Lawrence Livermore National Laboratory, P.O. Box 808, Livermore, CA 94551, USA

Received 17 December 2001; received in revised form 4 March 2002

Abstract

Various silica sols, with different surface chemistries, were reacted in solvent dispersions with hexamethyldisilazane (HMDS) or ethoxytrimethylsilane (ETMS) to produce hydrophobic, trimethylsilyl (TMS) functionalized sols. ^{1}H and ^{29}Si nuclear magnetic resonance were used to quantify the surface species and the TMS surface coverage. The amount of TMS surface coverage, which ranged from 5% to 33%, was a strong function of the starting silica-surface chemistry and the HMDS reaction time. Sols with a greater hydrogen-bonded silanol surface (as opposed to an ethoxy surface or isolated silanol surface) resulted in greater TMS coverage. HMDS reacts with both the solvent (ethanol) and the silica surface. Reaction rate measurements suggested that the silica surface reacts with HMDS at short times (minutes) and then with ETMS, which is a product of the HMDS/ethanol reaction, at long times (days). High TMS coverage is required for sol stability in non-polar solvents; the colloid size was found to increase in decane for sols with poor TMS coverage. In addition, coatings made from TMS sols showed an 80× slower remaining ethoxy-surface hydrolysis rate upon exposure to humidity than untreated sols. These TMS sol films will be utilized as anti-reflection coatings on moisture sensitive optics (e.g., potassium dihydrogen phosphate (KDP) crystals) used in high-peak-power laser systems.

© 2003 Published by Elsevier Science B.V.

1. Introduction

Colloidal silica (1 nm–1 μm) is used in a large number of applications in industries ranging from microelectronics to healthcare [1,2]. One method to create monodisperse silica sols, which was developed by Stöber more than 30 years ago, uses the sol–gel process [3]. In the Stöber process, silica particles are created by the hydrolysis and condensation of silicon alkoxides in alcohol solvents in the presence of a base (e.g., NH_3) and H_2O.

Colloidal silica made by the Stöber process is specifically attractive for use as anti-reflective (AR) coatings for optics used in high-peak-power laser systems because the colloids can be made with very low impurity levels, small particle size (~20 nm), and narrow particle size distributions [4–6]. These characteristics lead to coatings with low refractive indices, low scatter, and high laser

* Corresponding author. Tel.: +1-925 422 1884; fax: +1-925 423 0792.

E-mail address: suratwala1@llnl.gov (T.I. Suratwala).

0022-3093/03/$ - see front matter © 2003 Published by Elsevier Science B.V.
PII: S0022-3093(02)01629-0

damage thresholds, all of which are required for such laser systems [4,7]. These AR coatings work particularly well on silica glass optics. However, such coatings on KDP crystal optics (used for light frequency conversion) result in the formation of etchpits on the surface of the crystals. These etchpits are caused by water-enhanced dissolution of KDP due to capillary condensation of moisture within the coating [8]. The etchpits then cause optical scatter and hence have detrimental effects on laser performance. Water condensation in the coating is largely governed by the hydrophilic nature of the silica surface. Hence, one mitigation technique is to chemically modify the sol coating so that its surface is hydrophobic rather than hydrophilic, thereby minimizing water condensation and etchpit formation [8].

A silica surface can be made hydrophobic by chemical reaction (referred to as functionalizing, grafting, or silylating) with certain coupling agents to form trimethylsilyl (TMS, $-Si(CH_3)_3$) surfaces. TMS functionalization of silica surfaces has been previously accomplished by reaction with hexamethyldisilazane (HMDS) [9–18] or chlorotrimethylsilane [19–21] in the vapor phase. Zettlemoyer and Hsing [12] showed that TMS functionalization of silica colloids greatly altered the water adsorption isotherms, making them significantly more resistant to water adsorption. Others have shown that the degree of TMS coverage achieved is dependent on the type of surface silanols present (vicinal, geminal, or isolated) [9,11,15,19,20,22–24]. Vapor-phase surface modification, however, forms basic (NH_3) or acidic (HCl) products and requires the use of elevated temperatures to obtain high TMS coverage, all of which are harmful to the KDP surface. One way around this problem is to perform the silylation of the colloid in situ (i.e., while it is still in suspension) and then prepare the sol coating after harmful products have been removed by distillation. In situ TMS modification of various types of silica sols in various solvents has been recently accomplished using HMDS [8,25–27], trimethylalkoxysilanes [28], and trimethylhalosilanes [29].

In this study, HMDS was used as a trimethylsilylating agent to modify various Stöber silica sols in ethanol. The main objective was to determine and understand the parameters (e.g., surface chemistry and reaction time) that affect the amount of TMS coverage. Four different silica sols were synthesized by the Stöber process. These sols were treated with HMDS in solution to produce TMS functionalized colloids. Using ^{1}H and ^{29}Si magic angle spinning nuclear magnetic resonance (MAS NMR), the surface chemistry (i.e., isolated silanol, hydrogen-bonded silanol, and ethoxy species) of the four starting sols and the amount of TMS coverage of the HMDS treated sols were determined. Reaction rates of HMDS with the silica surface and with ethanol were also determined from NMR measurements. These data were used for determining the reaction mechanism and for developing methods to maximize TMS coverage. Next, the effects of the TMS functionalization on the properties and stability of the sol and of the sol-derived coatings were examined. Finally, the performance of TMS sols used as AR coatings on KDP optics was briefly evaluated.

2. Experimental

Six silica sols (labeled as Sols A–F) were synthesized. Sols A–D (referred to as starting sols) were used as precusors to prepare TMS-functionalized sols (Sols E and F). The reagents used were ethanol (dehydrated) (EtOH), concentrated ammonium hydroxide (Reagent Grade 28–30% NH_3) (NH_3(aq)), deionized water, tetraethoxysilane (Ultrapure Double Distilled Grade) (TEOS), ethoxytrimethylsilane (98%) (ETMS), decane (99+%, anhydrous, Aldrich), and HMDS.

Sol A: silica sol (3%) in ethanol. EtOH, NH_3(aq), and TEOS were mixed at a ETOH:NH_3:H_2O:TEOS mole ratio of 38:1:2.37:1 in the order listed above. A typical batch contained of 208 g TEOS, 59.4 g NH_3(aq), and 1732 g EtOH. The mixture was aged for three days at room temperature in a glass container without stirring before use. The resulting sol had 3 wt% SiO_2.

Sol B: silica sol (6%) in ethanol. This sol was prepared in the same manner as Sol A except that the ETOH:NH_3:H_2O:TEOS ratio was 16:0.13:2.5:1, and the sol was aged for 14 days. A typical batch contained of 208 g TEOS, 8.0 g NH_3(aq),

39.4 g H_2O, and 748 g EtOH. The resulting sol had 6 wt% SiO_2.

Sol C: silica sol (9%) in ethanol. This sol was prepared in the same manner as Sol A except that the TEOS:NH_3:H_2O:EtOH ratio was 9:0.06:2.5:1, and the sol was aged for 14 days. A typical batch contained of 208 g TEOS, 3.0 g NH_3(aq), 42.8 g H_2O, and 420 g EtOH. The resulting sol had 9 wt% SiO_2.

Sol D: silica sol (3%) in ethanol (refluxed). This sol was prepared by refluxing Sol A for ~8 h to remove NH_3 and H_2O. Refluxing was halted when a sample of the sol added to deionized water gave a pH less than 7. The resulting sol had 3 wt% SiO_2.

Sol E: HMDS treated sol (10%) in decane. The procedure for preparing Sol E is illustrated in Fig. 1, and the various processiong routes used are summarized in Table 4. This sol was prepared using one of the starting sols (Sols A–D). The starting sol was concentrated to 12 wt% SiO_2 by distilling off EtOH. H_2O in varying amounts (0–2.7 M) was often added, and the sol was aged for 12 h. Then HMDS was added in various amounts (0.75–1.5 M) and aged for 1–7 days. The solution was then diluted with decane (99+%, anhydrous, Aldrich) such that the TEOS:decane mole ratio is 1:3.8. Finally, all the components except for the decane and colloidal silica were removed by distilling until a temperature of 178 °C was reached. The resulting sol had 10 wt% SiO_2.

Sol F: ETMS treated sol (10%) in decane. EtOH from Sol B was removed by distillation until the silica concentration was 12 wt% SiO_2. Then ETMS and NH_3(aq) were added to the solution so that the ETMS:NH_4OH:TEOS mole ratio was 7.8:0.70:1. Then decane was added to obtain a TEOS:decane mole ratio of 1:3.8. Finally, all the components except for the decane and colloidal silica were removed by distilling until a temperature of 178 °C was reached. The resulting sol had 10 wt% SiO_2.

^{1}H and ^{29}Si MAS NMR. The samples for the solid state NMR measurements were prepared in two different manners. To characterize the sol, approximately 20 g each of Sol A–F were air-dried in glass weighing bottles for 1–3 days at room temperature. Some of the solid powder residue was heated at 120 °C for 8 h at 1 atm pressure. The resulting samples were measured using a 270 MHz Tecmag Airies NMR. ^{1}H MAS NMR measurements were conducted at 270 MHz with a spinning speed of 4.5 kHz, and pulse length and delay of 2 μs and 1 s, respectively. ^{29}Si MAS NMR measurements were conducted at 53 MHz with a spinning speed of 4 kHz, and pulse length and delay of 4 μs and 60 s, respectively.

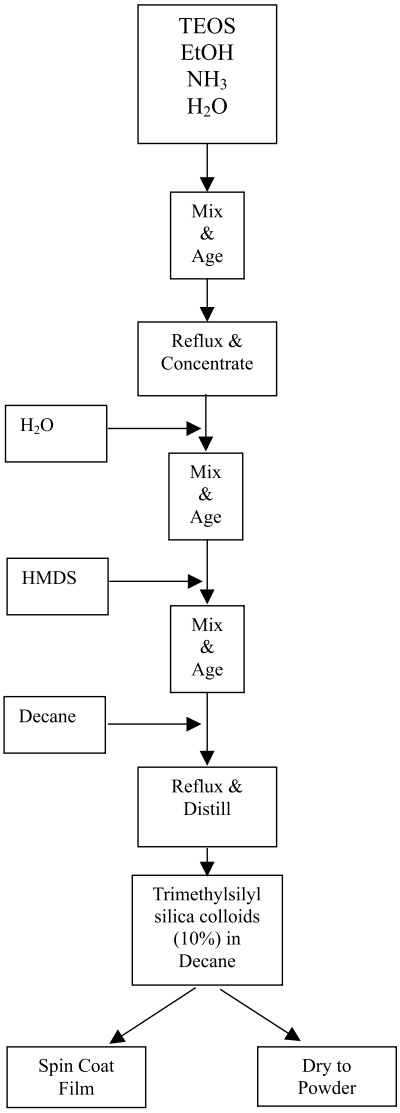

Fig. 1. Schematic of the preparation procedure for TMS functionalized silica sols (Sol E).

For the reaction rate measurements (i.e., to determine the amount of TMS coverage as a function of time), Sol E (after the HMDS was added to the sol) was vacuum dried while being heated in water bath at ~30–50 °C. The suspension dried to a solid powder within 8 min. Solid samples were prepared at various times after the HMDS was added, but prior to the decane addition. The resulting samples were measured using a 300 MHz Tecmag Airies NMR. ^{29}Si MAS NMR measurements were conducted at 53 MHz with a spinning speed of 4 kHz, and pulse length and delay of 4 μs and 60 s, respectively. 60 kHz proton decoupling was also used. Various delay times were first examined to ensure quantitative results.

^{1}H NMR. To determine the reaction rate of HMDS with EtOH, liquid ^{1}H NMR was performed at various times after HMDS addition during the preparation of Sol E. The sol was placed in a standard 5 mm NMR tube and measurements were conducted in a Brüker DRX 500 NMR using a 2 s delay. Neat samples were also analyzed to identify the chemical shifts.

Dynamic light scattering. Dynamic light scattering (DLS) measurements were carried out on a particle size analyzer. The sols were placed in a 1-cm pathlength plastic cuvette, and light scatter was measured at 90° in triplicate. The mean unimodal particle size was recorded. Details of the calculations of the particle size and standard deviation can be found elsewhere [30].

BET surface area. The sols were air-dried at room temperature and then vacuum dried at 80 °C for 24–48 h. Nitrogen adsorption was measured. The particle surface area was calculated using the Brunauer–Emmet–Teller (BET) model [31].

Colloid coatings. Two inch silicon wafers were coated with sol particles by spin coating. Approximately 1 ml of sol was dropped onto a spinning (1500–2400 rpm) Si wafer, and the coating was allowed to spread and dry for ~2 min. Coating thicknesses were ~2200 Å.

Transmission infrared spectroscopy. The water content of each sol was measured using an Fourier-transform infrared spectrometer. The sols were placed within a NaCl sealed cell with a 0.1 mm pathlength, and the absorbance at 1660 cm^{-1} was measured. The extinction coefficient of H_2O was measured using a series of standard solutions of H_2O in EtOH, which was determined as 28.5 l/(mole cm).

Reflectance infrared spectroscopy. The chemical composition of each coating was analyzed by infrared spectroscopy using a Fourier-transform infrared spectrometer (FTIR) with a variable-angle specular reflectance (VASR) unit. FTIR absorbance spectra were obtained by accumulating 500 scans over a frequency range 500–4600 cm^{-1} at a resolution of 1 cm^{-1}. The coated silicon wafers were supported so that coating was at the focus of the VASR. The spectrum of a bare silicon wafer substrate was subtracted from the spectrum of a coated wafer to obtain the spectrum of the coating. Changes in relative concentrations were monitored by measuring absorbance peak heights at characteristic frequencies: ethoxy species at 2975 cm^{-1} and TMS species at 2960 cm^{-1}. Between measurements, the coated wafers were stored in a hygrostat at 20 °C and 95% relative humidity.

3. Results and discussion

3.1. Surface chemistry of starting sols

Sols A–D were specifically prepared by different methods to alter the surface chemistry while maintaining approximately the same particle size. The compositions were chosen using an empirical relationship derived by Bogush et al., which allowed prediction of particle size according to the quantity of reagents used (TEOS, NH_3, and H_2O concentration) [32,33]. The properties of the sols are summarized in Table 1. The large surface area of the sols (400–600 m^2/g) suggests that the surface chemistry should play an important role in the properties and behavior of these sols.

The chemistry of silica surfaces has been previously studied, most notably by Maciel et al. using ^{1}H and ^{29}Si NMR [19,22,23,34–36]. The silica surface can include several types of chemical species. These include: (1) isolated silanols, (2) vicinal silanols, (3) geminal silanols, (4) siloxane bridges, (5) single ethoxy groups (6) geminal ethoxy groups, (7) vicinal ethoxy/silanol, and (8) TMS surfaces (Fig. 2). ^{1}H MAS NMR can be used to

Table 1
Basic properties of synthesized sols

Sol	Solvent	SiO_2 (wt%)	Mole ratio of starting composition[a]	Particle size (nm)	Water conc. (vol.%)	Solution density (g/cm^3)	pH	Solids loading (wt%)	BET surface area (m^2/g)	Refractive index of coating
A	EtOH	3%	1:1:2.37:38	22	0.92	0.802	10.5	3.5%	606	1.17
B	EtOH	6%	1:0.67:2:16	18	1.06	0.820	10.1	6.7%	557	1.20
C	EtOH	9%	1:0.06:2.5:9	26	1.43	–[b]	–[b]	–[b]	–[b]	1.17
D	EtOH	3%	1:1:2.37:38	6	0.25	0.838	6.9	3.5%	540	1.22
E	Decane	10%	na	25	0.96	0.785	8	13.0%	430	1.21
F	Decane	10%	na	28	–[b]	0.785	8	–[b]	–[b]	1.21

[a] TEOS:NH_3:H_2O:EtOH mole ratio.
[b] Not measured.

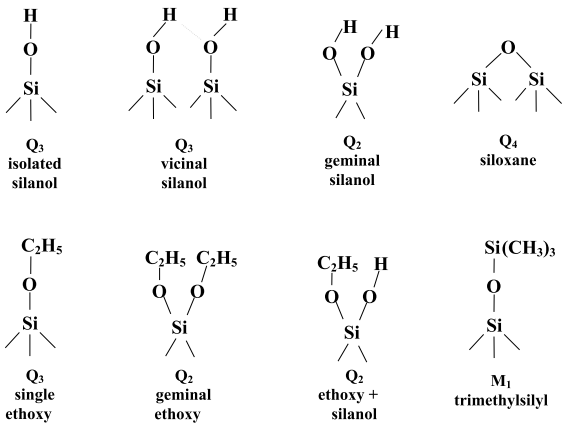

Fig. 2. Various types of surface species present on silica.

distinguish between many of these species on the surface of the colloid. Fig. 3 shows the ^{1}H MAS NMR spectra of Sols A–D after being dried 120 °C in air.

Five specific chemical shifts can be identified (peaks 1–5) as described in Table 2. The presence of the physisorbed water peak (~3.5 ppm) in these spectra suggests that heat treatment did not remove, at least permanently, all physisorbed species. The spectra also show the presence of isolated silanols (peak 2, 1.7 ppm), ethoxy groups (peaks 1 and 4, 1.0 and 3.7 ppm), and hydrogen bonded silanols (peak 5, 1–8 ppm –broad). Qualitatively the hydrogen bonded silanol concentration on the surface has the following Sol A > Sol B > Sol D > Sol C.

^{29}Si MAS NMR can be used to provide further insight into the silica surface chemistry as well as

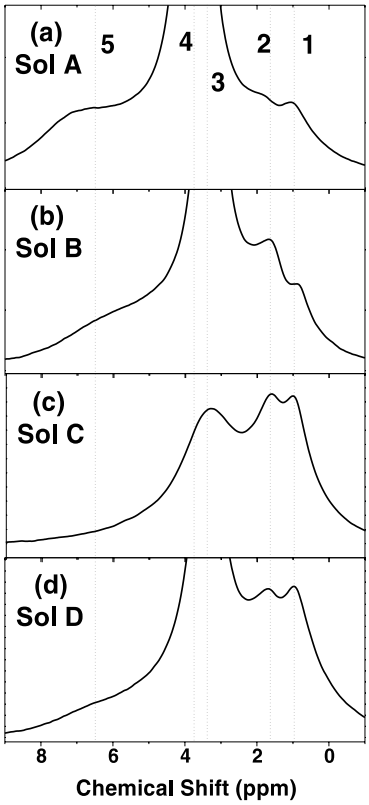

Fig. 3. ^{1}H MAS NMR spectra of Sols A–D after drying at 120 °C.

support some of the conclusions made using the ^{1}H MAS NMR data. This technique probes the local chemical environment around a Si atom. We use the following standard nomenclature to

Table 2
Identified ^{1}H MAS NMR chemical shifts of Sols A–D

Peak number	Chemical shift (ppm)	Chemical species	Reference
1	1.0	OCH_2CH_3	[44]
2	1.7	SiOH (isolated)	[19,35]
3	3.5	H_2O (physically absorbed)	[19,35,36]
4	3.7	OCH_2CH_3	[44]
5	1–8 (broad)	SiOH (hydrogen bonded)	[36]

describe the different silicate species: Q represents a quaternary oxygen tetrahedron; T represents a three-oxygen, one-alkyl-group tetrahedron; D represents a two-oxygen, two-alkyl-group tetrahedron; and finally M represents a one-oxygen, three-alkyl-group tetrahedron. In the current investigation, various Q species and M species (TMS species) are observed. The subscripts denote the number of alkoxide groups that have reacted to form Si–O–Si linkages. Therefore, Q_0 represents an unreacted TEOS precursor, and Q_4 represents a fully condensed silicate species. By the same token, M_0 represents an unreacted TMS group (such as ETMS, or hydroxytrimethylsilane) and M_1 represents an attached TMS group. The chemical shifts due to all these chemical species are well reported in the literature [19,20,22–24,37–39]. Based on reported values, the peaks were easily assigned as: Q_4 (−110 ppm), Q_3 (−102 ppm), Q_2 (−93 ppm), M_1 (12.5 ppm), M_0 (16 ppm) [20]. No Q_0 and Q_1 species were identified in the spectra.

^{29}Si MAS NMR spectra of the starting sols are shown in Fig. 4. These data shows that all the colloidal sols consist of Q_2, Q_3 and Q_4 species. The Q_2 species represent geminal silanol and/or ethoxy species, and Q_3 species represents the single silanols (either isolated or vicinal) and single ethoxy species (see Fig. 2). Quantitative analysis of the ^{29}Si MAS NMR spectra is reported in Table 3. Approximately 35–45% of the Q species are Q_2 and Q_3 species for these colloids (see Fig. 4). The majority of the surface species (>90%) in the starting sols constitute Q_3 species; hence the surface is dominated by single silanols (isolated and/or hydrogen bonded) and single ethoxy species.

Because these NMR experiments are conducted in the solid state, the peaks are broadened due to

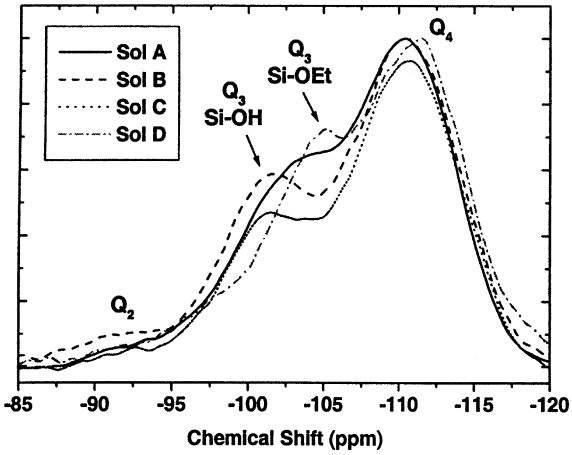

Fig. 4. ^{29}Si MAS NMR spectra of dried Sols A–D.

Table 3
Amount of various Q species in Sols A–D determined from data shown in Fig. 4

Sol	%Q_2	%Q_3	%Q_4
Sol A	3	35	63
Sol B	4	30	66
Sol C	2	30	68
Sol D	2	44	55

inhomogeneity caused by the various environments in which the Q species are located and by the type of Q species present. For example, there are two types of Q_3 species that can be present (single silanols or ethoxy). These two species have different chemical shifts that have been previously identified [40]. The single silanols (either isolated or vicinal) have a chemical shift of −100 ppm, and the single ethoxy surface have a chemical shift of −103 ppm. Fig. 4 identifies these specific chemical shifts. Note, however, we cannot distinguish between isolated and vicinal silanols from the ^{29}Si NMR data. The data on the starting sols suggest that the sols contain an silanol concentration with the following trend: Sol D < Sol C < Sol A < Sol B.

It is likely that the surface chemistry of the colloid is governed by its chemical environment (in this case, H_2O and ethanol concentration in solution). One can write the following simple overall equilibrium for the surface chemistry of the sol:

$$(Si-OEt)_S + H_2O \rightleftharpoons (Si-OH)_S + EtOH, \quad (1)$$

where the surface ethoxy concentration, $(Si–OEt)_S$, and surface silanol concentration, $(Si–OH)_S$, are determined by the relative H_2O and EtOH concentrations. Hence using Le Châtelier's principle [41], solutions that contain high concentrations of H_2O tend to have more silanol surface while solutions with low H_2O concentration tend to have more of an ethoxy surface.

Experimental evidence helps support this hypothesis. Sol A which had the greatest hydrogen bonded silanol content was prepared in solution containing the largest water concentration. By the same token, Sol D which had a low hydrogen bonded silanol content, had low water content in solution (compare Fig. 3 with Table 1). The only exception is Sol C, which has a high water concentration (1.4 vol.%), and it still had a noticeable ethoxy concentration on the surface. This may be due to the fact that the ammonia concentration was very low in this sol compared to Sols A and B. NH_3 most likely enhances the forward reaction by creating OH^- ions; note hydrolysis and condensation reactions are enhanced in basic environments [42]. If Eq. (1) is valid, then the addition of more H_2O to the sol, should result in further hydrolysis of the ethoxy surface. H_2O was added to Sol B and equilibrated for 24 h, and a dried sample was measured by ^1H MAS NMR (see Fig. 5). The results clearly indicate the removal of ethoxy groups (1.0 ppm) from the surface upon H_2O addition.

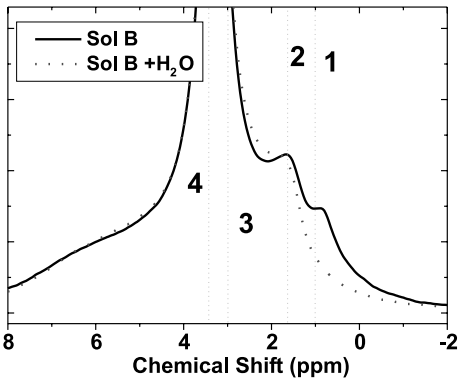

Fig. 5. ^1H MAS NMR spectra of Sol B with and without the addition of 2.7 M H_2O.

3.2. Effect of processing on the degree of TMS functionalization

Quantitative determination of the amount of TMS functionalization can be performed using ^{29}Si MAS NMR. Fig. 6(a) illustrates measured ^{29}Si MAS NMR spectra of Sol E made from Sols A–D. As the amount of TMS functionalization increases, the M_1 peak increases and Q_2 and Q_3 peak decrease. The same trend was observed by Linton et al. [20]. Also, one should expect an equivalent increase in Q_4 with increase in M_1. The amount of

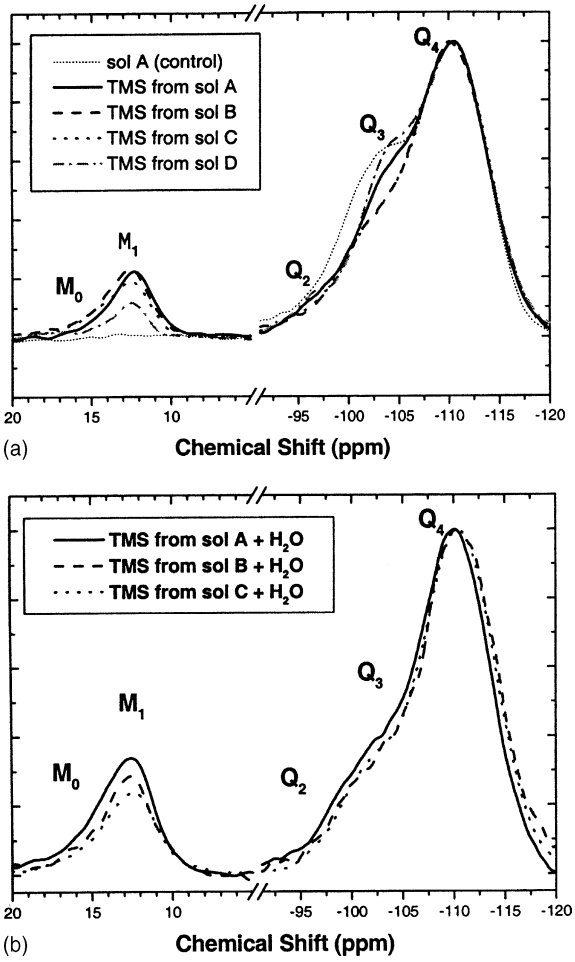

Fig. 6. ^{29}Si MAS NMR spectra; (a) of dried Sol E synthesized from Sols A–D. Sol E was synthesized using 1.5 M HMDS with a reaction time of two days (b) same as (a) except that 2.7 M H_2O was added to Sols A–D prior to HMDS addition.

TMS functionalization is quantified in two ways. First, we describe the TMS functionalization as the percentage of Si atoms in the colloid that have trimethyl groups attached, which is defined as

$$\theta_{Si} = \frac{A_{M1} \times 100\%}{A_{M1} + A_{Q1} + A_{Q2} + A_{Q3} + A_{Q4}}, \quad (2)$$

where A is the area of the peak in the ^{29}Si MAS NMR spectra of the specific silicate species identified in the subscript. The areas of the peaks were identified by deconvoluting the spectra using a standard Gaussian curve fitting routine. The TMS functionalization can also be quantified as the percentage of possible reactable surface sites functionalized, which is defined as

$$\theta_S = \frac{A_{M_1} \times 100\%}{A_{M_1} + A_{Q1} + A_{Q_2} + A_{Q_3}}. \quad (3)$$

In this calculation of the TMS surface coverage, we assume that only one site of a geminal species (Q_2) can react with HMDS due to steric hindrance.

Table 4 lists the various processing routes utilized to produce Sol E (TMS functionalized sol). In the table, the specific processing variables have been identified, and the amount of TMS functionalization is reported as calculated by Eqs. (2) and (3). Careful examination of Table 4 reveals a number of relevant processing variables that affect the amount of TMS coverage.

The type of starting sol used had a strong effect on the TMS coverage (see Fig. 6(a) and Table 4). Samples 3, 9, 12 and 14 all had the same processing route but different starting sols (no added water, 1.5 M HMDS, two days reaction time). By comparing this set of samples, we see that Sol D produced the worst TMS functionalization ($\theta_S = 13\%$), and Sol B produced the best TMS functionalization ($\theta_S = 22\%$). Sol D had the least silanol surface and Sol B had the largest silanol surface. HMDS will react with a silanol surface site, but not with an ethoxy surface site.

In order to further improve the TMS coverage, water was added to some of the starting sols to hydrolyze the ethoxy surface (see Eq. (1)). The effect of water on the surface chemistry is shown by examining Fig. 5, which shows the ^{1}H MAS NMR spectra before and after water addition. Fig. 6 shows the ^{29}Si MAS NMR spectra of Sol E using precursor sols (Sol A, B, or C) with and without added H_2O. A noticeable improvement in the

Table 4
Different processing routes for producing Sol E

Sample	Starting sol	Added [H_2O] (M)	[HMDS] (M)	HMDS reaction time (days)	(θ_{Si}) % TMS of total Si in colloid	(θ_S) % TMS of reactable sites
1	Sol A	0	0.75	1	5.0	13.3
2	Sol A	0	0.75	3	5.3	14.5
3	Sol A	0	1.5	2	5.7	14.7
4	Sol A	2.7	1.5	2	9.7	28.0
5	Sol A	2.7	1.5	7	11.3	31.2
6	Sol B	0	0.75	1	5.4	16.6
7	Sol B	0	0.75	3	6.1	24.8
8	Sol B	0	0.75	7	8.1	32.6
9	Sol B	0	1.5	2	6.2	22.2
10	Sol B	0.54	1.5	2	7.0	23.4
11	Sol B	2.7	1.5	2	9.3	32.6
12	Sol C	0	1.5	2	4.8	14.6
13	Sol C	2.7	1.5	2	7.7	25.9
14	Sol D	0	1.5	2	5.0	13.0
15	Sol D	0	0.75	1	3.7	5.4
16	Sol B	0	Vapor treatment	–	5.3	17.2

Table illustrates effect of starting sol, H_2O concentration, HMDS concentration and reaction time on the amount of TMS coverage.

TMS coverage was obtained for all the starting sols (Sols A, B, and C) upon H_2O addition. Adding H_2O to Sol A increased θ_S of Sol E from 14.7% to 28.0%; adding H_2O to Sol B increased θ_S of Sol E from 22.0% to 32.6%; and adding H_2O to Sol C increased θ_S of Sol E from 14.6% to 25.9%.

The silanol species are the reactive site for TMS functionalization; however, the exact type of silanol species (geminal, isolated, or vicinal) that is the most reactive species is a more difficult question to answer. Numerous groups have sought the answer to this question using vapor treatment of various trimethylsilylating agents [9,10,16,19,20,23,24,34]; however, there is much discrepancy in the results and conclusions. Some report that isolated single silanols are the most reactive surface site to HMDS and chlorotrimethylsilane [9,11,22]. Others have reported that geminal and/or hydrogen boded silanols are more reactive [10,19,23,43]. Using ^{29}Si NMR Linton argued that surface modification resulted in the decrease first in the Q_2 peak and then Q_3 peaks. Hence, geminal silanols were most reactive followed by single silanols (most likely hydrogen-bonded) [20]. Kytokivi [10] used reflectance IR in the low frequency region to show a significant amount of isolated silanols (960 cm^{-1}) after HMDS vapor treatment, suggesting that the isolated silanols were unreactive with the HMDS.

The results from the present study can provide some insights to different reactivities of various silanol sites. First, note that our functionalization reactions were performed in solution, not in the vapor phase, which could have a large impact on surface site reactivity. Therefore, it is risky to compare our work with vapor treatment studies on surface site reactivity. Fig. 6(b) shows the ^{29}Si MAS NMR spectra of three different sols synthesized from Sol A–C with H_2O added. All these starting sols had most of the ethoxy groups hydrolyzed, and should only have isolated and hydrogen-bonded silanol surface. Sol A (which had the highest hydrogen bonded silanol concentration) had the highest absolute amount of TMS ($\theta_{Si} = 15.4\%$) in the sol while Sol C (which had the lowest hydrogen bonded concentration) had the least absolute amount of TMS coverage ($\theta_{Si} = 10.3\%$) in the sol in that series. Hence, it appears that TMS functionalization occurs more efficiently on sols containing more hydrogen bonded silanols. This is not an unreasonable conclusion. Isolated silanols are isolated either because they are in closed pores or are shielded by species that prevent other H containing species from interacting with them [36]. If a small chemical species such as H_2O can not interact with the isolated silanol, it is hard to believe that a molecule large as HMDS can. Also, hydrogen-bonded silanols are more acidic (proton donor) and are more likely to react.

The reaction time after HMDS is added to the starting sol also affected the amount of TMS coverage. This is most clearly illustrated with Sol B as the starting sol (Samples 6, 7 and 8 in Table 4). The same trend is observed by comparing samples 4 and 5. Increasing the reaction time up to seven days appears to have increased the amount of TMS. More details on the reaction time and reaction mechanism are discussed in the next section.

Finally, we compare the difference between HMDS vapor treatment with that of HMDS solution treatment with respect to TMS coverage. Using the solution treatment, various amounts of TMS coverage have been achieved, $\theta_S = 5$–33%. Using a vapor-phase treatment protocol described by Thomas et al. [18], room temperature vapor HMDS of Sol A gives $\theta_S = 17\%$. These results indicate that with proper processing, greater TMS coverage can be achieved using HMDS solution treatment.

3.3. Reaction rate and mechanism of TMS functionalization

During the synthesis of Sol E, a large excess of HMDS had to be added in order to get significant TMS coverage. In fact, only 0.23 M-HMDS is theoretically needed to obtain 100% TMS coverage, while 1.5 M HMDS is typically used. The reason for this is that HMDS reacts with EtOH (which is the solvent) as well as the silica surface. Although using HMDS in an ethanol based system seems wasteful, it is more economical to use excess HMDS than to perform a solvent exchange or to develop a new silica sol system for the purpose of making AR coating for high-peak power lasers.

The following reaction scheme is proposed:

$$(CH_3)_3Si{-}\underset{\underset{H}{|}}{N}{-}Si(CH_3)_3 + 2CH_3CH_2OH \xrightarrow{k_1} 2CH_3CH_3O{-}Si(CH_3)_3 + NH_3, \quad (4)$$

$$(CH_3)_3Si{-}\underset{\underset{H}{|}}{N}{-}Si(CH_3)_3 + 2{\equiv}Si{-}OH \xrightarrow{k_2} 2{\equiv}Si{-}O{-}Si(CH_3)_3 + NH_3. \quad (5)$$

HMDS can react with ethanol to produce ETMS or with the silanol surface to produce a TMS modified surface: k_1 and k_2 are the reaction rate constants for Eqs. (4) and (5), respectively. In both reactions, ammonia is created. The reaction rates of Eqs. (4) and (5) were probed using ^{1}H and ^{29}Si NMR upon the addition of HMDS into the starting sol solution (Sample 6 in Table 4). ^{1}H solution NMR spectra showed numerous peaks from protons in H_2O (OH, ~5.0 ppm), HMDS ($Si(CH_3)_3$, −0.016 ppm) EtOH (CH_3, 1.1 ppm; CH_2, 3.52 ppm), and ETMS ($Si(CH_3)_3$, 0.025 ppm; CH_2, 3.58; CH_3, 1.1 ppm). The ETMS and HMDS concentration were determined by the increase in the ETMS chemical shifts (0.025 ppm, 3.58 ppm) and the decrease in the HMDS peak (−0.016 ppm). The calculated concentrations of HMDS and ETMS are shown as a function of time in Fig. 7(a). The reaction of HMDS with ethanol appears to follow a simple first order reaction and hence the concentrations of HMDS (C_{HMDS}) and ETMS (C_{ETMS}) as a function of time (t) can be simply described as

$$C_{HMDS}(t) = C_o e^{-k_1 t}$$
$$C_{ETMS}(t) = 2C_o(1 - e^{-k_1 t}) \quad (6–7)$$

where C_o is the original HMDS concentration and k is the reaction rate constant. The best fit to the data gives $k_1 = 1.95 \times 10^{-3}$ s^{-1}. The half life ($t_{1/2}$) of the HMDS is very short, only 6 min. Also, note that basically all the HMDS reacts with EtOH since 1.5 M creates approximately 3.0 M-ETMS.

The HMDS/silanol surface reaction could not be determined from the ^{1}H NMR data due to the large concentrations of the HMDS/EtOH reaction species. To monitor the TMS coverage of the silica surface, a portion of the sol was removed at various times after the additon of HMDS. The sample

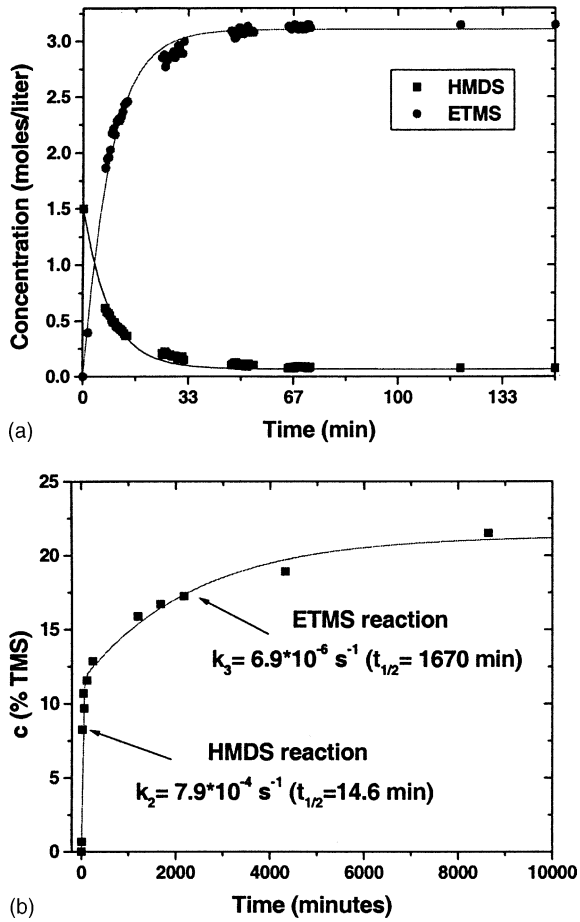

Fig. 7. (a) HMDS and ETMS concentration as a function of time as determined by ^{1}H solution NMR; (b) TMS coverage (θ_S) as a function of time after HMDS addition as determined by ^{29}Si MAS NMR on vacuum dried samples.

was then vacuum dried and analyzed by ^{29}Si MAS NMR. Fig. 7(b) shows the calculated TMS coverage (using Eq. (3)) as a function of time. The TMS coverage rate (shown in Fig. 7(b)) appears to have two components: a fast reaction occurring within the first hour and a slower reaction which takes place on the order of days. The fast reaction is likely due to the HMDS/silanol surface reaction (Eq. (5)). Because essentially all the HMDS is consumed within the first 30 min (Fig. 7(a)), the slow reaction is not likely due to the HMDS/silanol surface reaction. One likely explanation is that the by-product of the HMDS/EtOH reaction, ETMS, reacts with the silanol surface as follows:

$$(CH_3)_3Si{-}OCH_2CH_3 + \equiv Si{-}OH \xrightarrow{k_3} \equiv Si{-}O{-}Si(CH_3)_3 + CH_3CH_2OH. \quad (8)$$

To test whether ETMS can react with the silica surface, Sol F was synthesized. NH_4OH was added as a catalyst. The resulting amount of TMS functionalization was $\theta_S = 19.7\%$ as measured by ^{29}Si MAS NMR. This result indicates ETMS can participate in the TMS functionalization of the silica surface, suggesting that this reaction is the probable explaination for the slow TMS functionalization rate at long times in Fig. 7(b).

The set of reactions (Eqs. (4), (5), and (8)) can be used to describe the kinetics of overall TMS coverage rate. Since, $k_1 \gg k_3$, we can simply describe the TMS coverage rate as

$$\theta_s(t) = \theta_{s_{HMDS}}(1 - e^{-k_2 t}) + \theta_{s_{ETMS}}(1 - e^{-k_3 t}), \quad (9)$$

where $\theta_{s_{HMDS}}$ is the maximum TMS coverage due to Eq. (5), and $\theta_{s_{ETMS}}$ is the maximum TMS coverage due to Eq. (8). Note k_2 is actually a composite of the consumption of HMDS in the intrinsic HMDS–SiOH reaction (Eq. (5)) and in the HMDS–EtOH reaction (Eq. (4)). In other words, the HMDS–SiOH reaction rate decreases because HMDS concentration is reduced by the HMDS–ETOH reaction. The best fit of Eq. (9) is shown in Fig. 7(b) with $k_2 = 7.9 \times 10^{-4}$ s^{-1} and $k_3 = 6.9 \times 10^{-6}$ s^{-1}. $\theta_{s_{HMDS}}$ was determined as 12% and $\theta_{s_{ETMS}}$ was determined as 10%. Hence a significant amount of TMS coverage occurs from both HMDS and ETMS reacting with the silica surface.

Based on the results of the kinetic analysis, the TMS coverage is maximized by allowing Sol E to sit for at least seven days after the addition of HMDS. The data in Table 4 also support this conclusion.

3.4. Effect of surface chemistry on sol stability in non-polar solvents

Upon the addition of HMDS during the synthesis of Sol E, the colloid surface changes from a hydrophilic (silanol) surface to a hydrophobic (TMS) surface. The amount of TMS coverage is essentially describing the degree of hydrophobicity of the surface. The colloid stability of the TMS sols in non-polar solvents was found to be a strong function of the TMS coverage. The TMS sol which was originally in ethanol (a hydrophilic solvent) was transferred to decane (a hydrophobic solvent). Fig. 8(a) shows the hydrodynamic particle size of the colloid as a function of time after Sol E was transferred into decane for sols with varying degrees of TMS coverage. Also, as shown in Fig. 8(b), the difference in particle size of the TMS sols is illustrated by the change in optical transparency due to an increase in optical scatter with increase

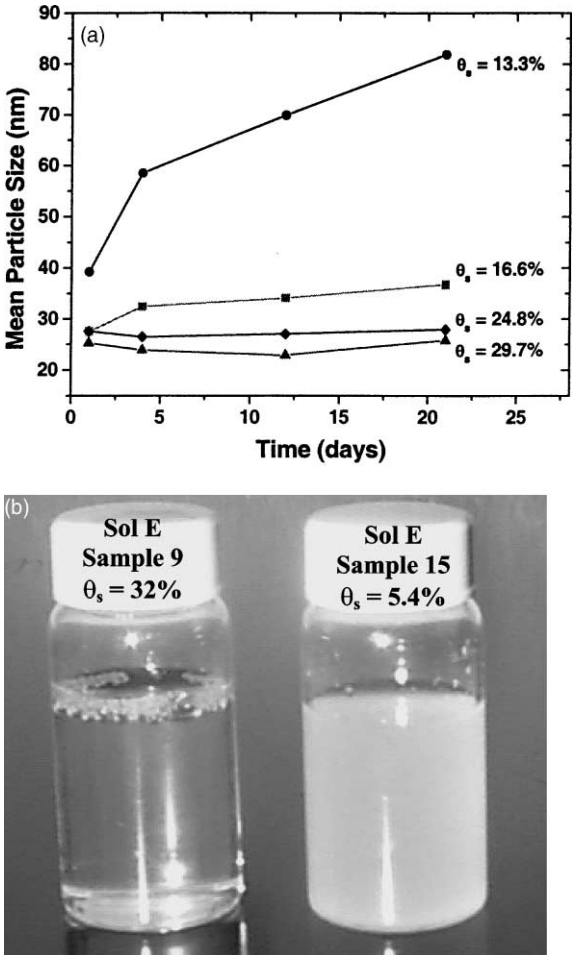

Fig. 8. (a) Effect of TMS coverage of Sol E on the temporal stability of the colloid size. The hydrodynamic particle size was measured by DLS; (b) Photograph of two TMS functionalized sols (Sol E), one with high TMS coverage ($\theta_S = 33\%$) and one with low TMS coverage ($\theta_S = 5.4\%$).

in particle size. The sols with low TMS coverage resulted in an increase in particle size, while those with a TMS coverage greater than $\theta_S = 25\%$ were stable. A sol with coverage less than this level must still have a portion of the colloid exposed with a hydrophilic surface, and hence such a colloid in a hydrophobic solvent (e.g., decane) is unstable and will start to aggregate with other colloids having a hydrophilic surface. At TMS coverage of $\theta_S \geqslant 25\%$, the TMS groups must sterically hinder (i.e., act as an umbrella) the interaction of any remaining silanols on the colloid surface.

3.5. Effect of surface chemistry on colloid coating stability

The chemical stability of the sols after being cast as films is also a strong function of surface species. As films, the colloids essentially stack up like random billiard balls on the surface of the substrate. Three films from Sols A, D, or E were exposed to 95% humidity, and the surface chemsitry was evaluated by reflectance infrared spectroscopy. The hydrocarbon vibrations were monitored as a function of time (ethoxy at 2975 cm^{-1} and TMS at 2960 cm^{-1}). The results are shown in Fig. 9. Note that at time zero, Sol D (refluxed sol) has the largest amount of ethoxy groups, followed by Sol A (3% sol), and then by Sol E (TMS sol). Upon exposure of the coatings to moisture, the ethoxy absorbance for all three coatings decreases due to ethoxy hydrolysis resulting in the formation of silanols. Also, for Sol E, the TMS coating, the TMS vibration (2960 cm^{-1}) was found not to change within the error of the measurement (see Fig. 9(b)).

The rate of the ethoxy hydrolysis varied dramatically depending on the starting surface chemistry of the colloids. The rate of hydrolysis follows a simple first-order reaction rate (i.e., data fits a single exponential decay with time). The rate of hydrolysis was fastest ($t_{1/2} = 1.4$ days) for Sol A, which initially had the highest silanol surface. The rate of hydrolysis of Sol D, which originally had more of an ethoxy surface, was about $5\times$ slower. Finally, the rate of the ethoxy group hydrolysis in the TMS sol was the slowest ($\sim 80\times$ slower than Sol A). Clearly, the hydrophobic na-

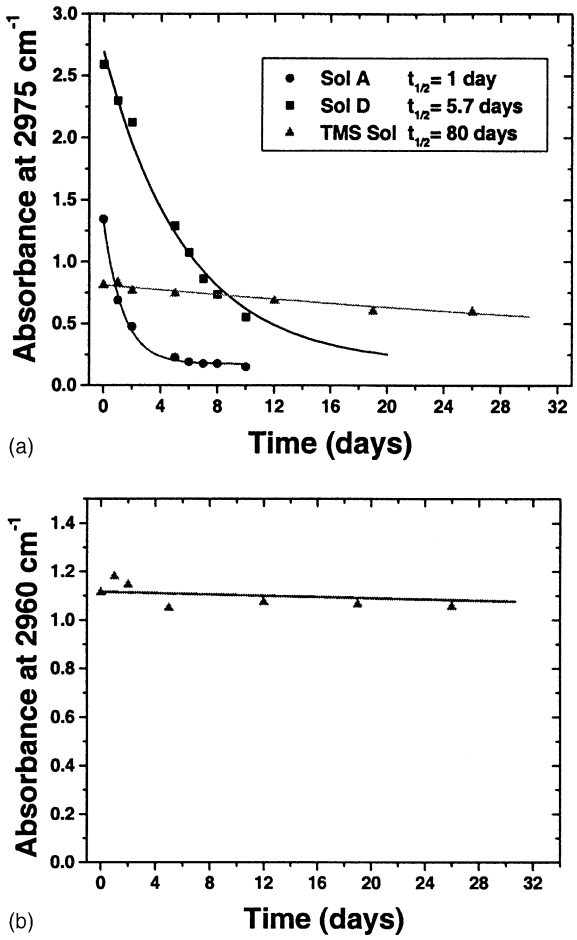

Fig. 9. (a) Reflectance IR absorbance at 2975 cm^{-1} due to ethoxy groups on the surface of colloidal films (Sols A, D and E) as a function of time of exposure to 95% relative humidity atmosphere; (b) Reflectance IR absorbance at 2960 cm^{-1} due to TMS groups on the surface of colloidal films as a function of time of exposure to 95% relative humidity atmosphere.

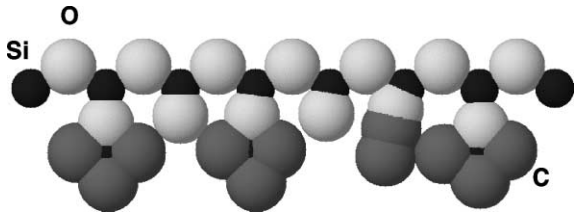

Fig. 10. Space fill illustration of the surface chemistry of silica colloid having TMS, ethoxy, and silanol surface. Note H atoms are not shown for simplicity.

ture and the steric effects of the trimethysilyl group must inhibit the penetration of H_2O to the ethoxy groups. Fig. 10 illustrates the potential steric effect of the ethoxy and, more so, the TMS groups on the silica surface.

3.6. Maximum TMS coverage, hydrophobicity, and KDP etchpit prevention

The surface site density can be estimated for each of the silica colloids (Sols A–D) using a relationship given by Maciel [23] as

$$S = f_g 7.9\ \mathrm{nm}^{-2} + (1 - f_g)4.6\ \mathrm{nm}^{-2}, \qquad (10)$$

where f_g is the fraction of the surface sites that are geminal species (Q_2). f_g can be easily calculated using the data in Table 3. It turns out that all the colloids have a very similar number of reactable sites with $S = 4.8 - 4.9\ \mathrm{nm}^{-2}$. The maximum TMS surface coverage achieved was about $\theta_s = 30$–33%. Hence the TMS site density is 1.6 nm^{-2}.

For a dense, spherical colloid with a 20 nm diameter, the theoretical surface area would be ~310 m^2 /g, which is about 40–50% of the surface area that is measured (see Table 1). Hence one would expect about half of the surface area should be found on the open and closed pores inside the colloid. The relatively large-sized HMDS and ETMS molecules likely have difficulty penetrating into the open pores of the colloid and can not penetrate into the closed pores. These surfaces will not be modified. If we assume all the open pores and closed pore contain unreachable surface sites, then the surface coverage becomes 55–66% of reactable sites, or 2.7–3.2 nm^{-2}. Maciel [23] calculated a theoretical surface site density, which is limited by steric hindrance, as high as 2.8 nm^{-2}. Therefore, the maximum TMS coverage achieved in this study corresponds near the maximum achievable coverage with a steric limitation.

The selection of the process that provides the maximum TMS coverage depends on which parameter for TMS coverage is used (θ_{Si} or θ_S). Sol E (sample 5) had the highest absolute amount of TMS groups on the surface ($\theta_{Si} = 11.3\%$) where as Sol E (sample 11) had the greatest fraction of the reactable sites with TMS groups ($\theta_S = 32.6\%$). In general, Sol E samples synthesized from Sol A had higher values for θ_S for an equivalent value of θ_{Si} compared to Sol E samples synthesized from Sol B (see Fig. 11). The reason for this difference is likely due to the amount of internal porosity (either open pores that are inaccessible to the silylating agent or closed pores). Sols A and B have nearly the same colloid size, but Sol B has a lower surface area and cast films from this sol have a higher refractive index. Sol B likely contains denser SiO_2 particles with less internal porosity. Therefore, one would expect Sol E made from Sol B to have a greater θ_S for an equivalent amount of θ_{Si}.

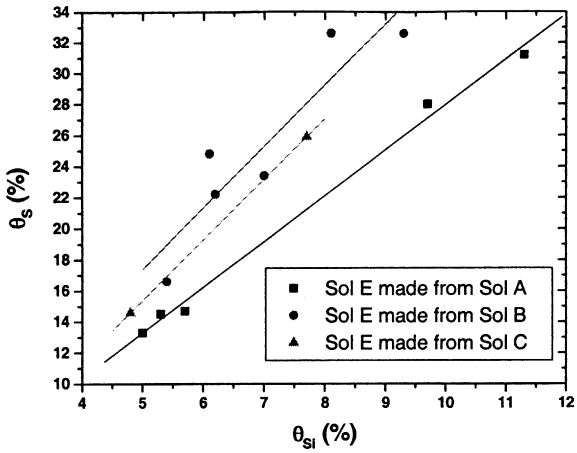

Fig. 11. Percentage of reactable sites that were modified by TMS (θ_S) vs percentage of total that Si that were modified by TMS (θ_{Si}) for different starting sols. The lines represent a best-fit linear regression of the data for each of the starting sols.

As described in the introduction, the driving force for making a TMS sol was to make a hydrophobic coating that would prevent etchpit formation on KDP optics. To illustrate the hydrophobic nature of the TMS sol, the macroscopic wetting characteristics of the coating were examined. Sol B and Sol E (sample 11) were spin coated on a silicon wafer and a water droplet was placed on top. The great difference in contact angle illustrates the highly hydrophobic nature of the Sol E coating (see Fig. 12). Sol E was also successful in preventing etchpit formation on KDP. This is illustrated in Fig. 13, which shows the optical scatter for a Sol A and Sol E coating on KDP upon storing in 55% relative humidity for long times. The greatly reduced optical scatter in the TMS coating is due to the lack of etchpit

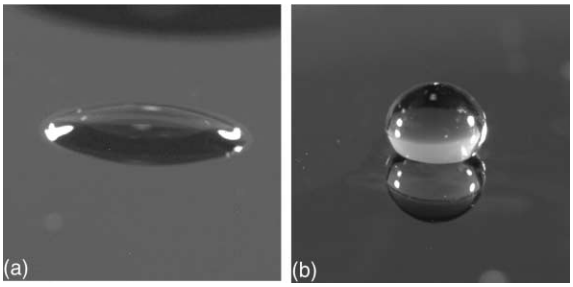

Fig. 12. Photograph of a water droplet on (a) Sol B and on (b) Sol E. The difference in wetting is a result of a highly hydrophilic silanol surface (Sol B) versus a hydrophobic, TMS surface (Sol E).

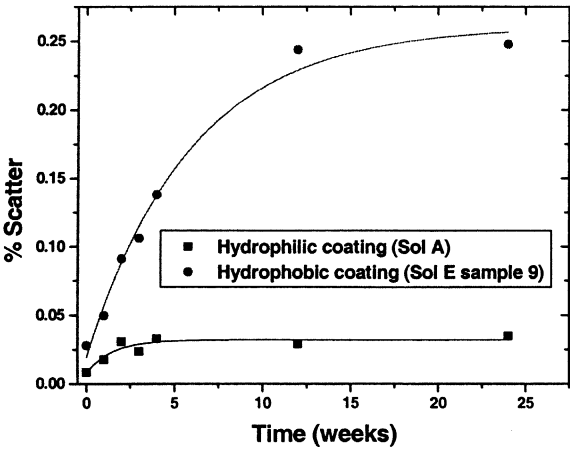

Fig. 13. Optical scatter from sol coating (Sol A or Sol E) on a KDP optic upon storing the optic at 55% relative humidity as a function of time. The lines represent exponential fits to the data and are a guide for the eye.

formation on the KDP surface [17]. The importance of the rate of ethoxy hydrolysis is also correlated to etchpit formation when these sols are coated on KDP [8]. It was found that etchpit formation kinetics on KDP had rates that followed this trend: sol A > sol D ≫ sol E, following the same trend as the ethoxide hydrolysis (see Fig. 9(a)).

4. Conclusions

The surface chemistry of Stöber silica colloids can be varied dramatically by changing the relative quantities of the starting reagents used to make the sol and by modifying the solvent environment around the sol. HMDS can be reacted with these silica sols in suspension to produce very hydrophobic, TMS functionalized sols. The variation in starting surface species, the HMDS reaction time, and concentration all strongly affect the amount of TMS coverage that takes place. HMDS appears to prefer to react with hydrogen bonded silanols, and the maximum TMS coverage achieved corresponds well to the maximum theoretical coverage calculated based on the size of the TMS group. The TMS functionalization of the silica sol greatly increases the hydrophobicity and stability of the sol in non-polar solvents, and films cast from this sol serve to prevent etchpit development on KDP optics.

Acknowledgements

The work was performed under the auspices of the US Department of Energy by Lawrence Livermore National Laboratory under contract No. W-705-Eng-48. The authors would like to thank G. Turner at Spectral Data Services for performing much of the NMR measurements, and S. Hulsey for performing the BET surface area measurments. The assistance of A. Flammini in the preparation of this manuscript is also greatly appreciated.

References

[1] R. Iler, The Chemistry of Silica, John Wiley, New York, 1979.
[2] H.E. Bergna, Colloid Chemistry of Silica, American Chemical Society, DuPont, Wilmington, DE, 1994.
[3] W. Stober, A. Fink, E. Bohn, J. Colloid Interf. Sci. 26 (1968) 62.
[4] I.M. Thomas, Appl. Opt. 25 (1986) 1481.
[5] J.R. Murray, SPIE 3492 (Supplement) (1998) 1.
[6] M. Andre, M. Novaro, D. Schirmann, Chocs Rev. Sci. Techn. Direct. Appl. Milit. 13 (1995) 73.
[7] I. Thomas, SPIE 2114 (1993) 232.
[8] E.K. Wheeler, J.T. McWhirter, P.K. Whitman, C. Thorsness, J. DeYoreo, I.M. Thomas, M. Hester, SPIE 3902 (1999) 451.
[9] W. Hertl, M.L. Hair, J. Phys. Chem. 75 (1971) 2181.
[10] A. Kytokivi, S. Haukka, J. Phys. Chem. 101 (1997) 10365.

[11] S. Hauuka, E.L. Lakomaa, T. Suntola, Appl. Surf. Sci. 82&83 (1994) 548.
[12] A.C. Zettlemoyer, H.H. Hsing, J. Colloid Interf. Sci. 58 (1977) 263.
[13] B. Boddenberg, R. Grosse, U. Breuninger, Surf. Sci. 173 (1986) L655.
[14] A. Varvarin, L. Belyakova, V. Tertykh, L. Lazukina, V. Kukhar, Theor. Exp. Chem. 24 (1989) 482.
[15] V.V. Brei, J. Appl. Spectrosc. 56 (1992) 205.
[16] B. Morrow, A. McFarlan, in: H. Bergna (Ed.), The Colloid Chemistry of Silica, vol. 234, American Chemical Society, Washington DC, 1994, p. 183.
[17] P.K. Whitman, J. Fair, R. Aboud, A.K. Burnham, S.C. Frieders, I.M. Thomas, C.B. Thorsness, UCRL-LR-105821-99-2, 1999.
[18] I.M. Thomas, A.K. Burnham, J.R. Ertel, S.C. Frieders, SPIE 3492 (1998) 220.
[19] G.E. Maciel, C.E. Bronnimann, R.Z. Zeigler, I. Chuang, D.R. Kinney, E. Keiter, in: H. Bergna (Ed.), The Colloid Chemistry of Silica, vol. 234, American Chemical Society, Washington DC, 1994, p. 269.
[20] R.W. Linton, M.L. Miller, G.E. Maciel, B.L. Hawkins, Surf. Interf. Anal. 7 (1985) 196.
[21] R.K. Iler, US Patent 2,801,185, 1957.
[22] S. Haukka, A. Root, J. Phys. Chem. 98 (1994) 1696.
[23] D. Sindorf, G. Maciel, J. Phys. Chem. 86 (1982) 5208.
[24] D. Sindorf, G. Maciel, J. Phys. Chem. 87 (1983) 5516.
[25] J.T. Hunt, UCRL-ID-138120-99, Lawrence Livermore National Laboratory, 2000.
[26] G.T. Burns, Q. Deng, J.R. Hahn, T.G. Krivak, T.A. Okel, C.C. Reese, US Patent 6,184,408, 1999.
[27] P.J. Griffith, W. Herron, B.R. Harkness, R.M. Taylor, D.J. Wilson, US Patent 5,919,298, 1998.
[28] K. Yoshitake, T. Yokoyama, US Patent 6,025,455, 2000.
[29] V.C. Menon, J. Paul, D.M. Smith, K.C. Keohlert, US Patent 6,174,926, 1999.
[30] Coulter N4 Plus Submicron Particle Sizer: Reference Manual, Coulter Corporation, Miami, FL, 1995.
[31] S. Gregg, K. Sing, Adsorption Surface Area, and Porosity, Academic Press, London, 1967.
[32] G.H. Bogush, M.A. Tracy, I.C.F. Zukoski, J. Non-Cryst. Solids 104 (1988) 95.
[33] G.H. Bogush, I.C.F. Zukoski, J. Colloid Interf. Sci. 142 (1991) 1.
[34] D. Sindorf, G. Maciel, J. Am. Chem. Soc. 105 (1983) 3767.
[35] C. Bronnimann, R. Zeigler, G. Maciel, J. Am. Chem. Soc. 110 (1988) 2023.
[36] C. Liu, G. Maciel, J. Am. Chem. Soc. 118 (1996) 5103.
[37] R. Glaser, G. Wilkes, C. Bronnimann, J. Non-Cryst. Solids 113 (1989) 73.
[38] W. Klemperer, V. Mainz, D. Millar, Mater. Res. Soc. Symp. 73 (1986) 15.
[39] F. Babonneau, New J. Chem. 18 (1993) 1065.
[40] H.G. Horn, H.C. Marsmann, Makromol. Chem. 162 (1972) 255.
[41] S. Zumdahl, Chemistry, D.C. Heath and Company, Lexington, Massachusetts, 1986.
[42] C. Brinker, G. Scherer, Sol-Gel Science, Academic Press, Inc, Boston, 1990.
[43] L.R. Snyder, Sep. Sci. 1 (1966) 191.
[44] C. Pouchert, Aldrich Library of NMR Spectra, 2nd Ed., Aldrich, Milwaukee, WI, 1983.